

electrons (this is discussed later in the present paper).

- <sup>1</sup>S. F. Edwards, *Philos. Mag.* **3**, 1020 (1958).  
<sup>2</sup>S. Titeica, *Ann. Phys. (Leipzig)* **22**, 129 (1935); E. N. Adams and T. D. Holstein, *J. Phys. Chem. Solids* **10**, 254 (1959).  
<sup>3</sup>R. Kubo, H. Hasegawa, and N. Hashitsume, *J. Phys. Soc.*

- Jpn.* **14**, 56 (1959).  
<sup>4</sup>V. V. Popov and A. V. Chaplik, *Zh. Eksp. Teor. Fiz.* **73**, 1009 (1977) [*Sov. Phys. JETP* **46**, 534 (1977)].  
<sup>5</sup>O. V. Romanov, V. Ya. Uritskii, and A. M. Yafasov, *Fiz. Tekh. Poluprovodn.* **10**, 332 (1976) [*Sov. Phys. Semicond.* **10**, 198 (1976)].

Translated by A. Tybulewicz

## Dependence of the effects of spatial dispersion in a crystal on the exciton-damping constant

M. I. Strashnikova and E. V. Besonov

*Physics Institute, Ukrainian Academy of Sciences*  
(Submitted 21 December 1977)  
*Zh. Eksp. Teor. Fiz.* **74**, 2206–2214 (June 1978)

We calculate the spectral dependences of the optical constants of two normal waves due to the spatial dispersion of  $\epsilon$  in the region of the lowest excitonic state of a CdS crystal at different values of the damping constant  $\gamma$ . The obtained curves are used for a quantitative estimate of  $\gamma$  in real crystals. Two branches of the refractive index within the limits of the absorption band are measured by a direct interference method for a CdS crystal whose  $\gamma$  is close to the "critical" value.

PACS numbers: 78.20.Dj

### INTRODUCTION

Pekar formulated theoretically in 1957<sup>[1]</sup> the main premises of crystal optics in the region of the exciton absorption bands, when spatial dispersion of the dielectric constant  $\epsilon(\omega, \mathbf{k})$  becomes significant. In contrast to classical optics, which takes no account of the dependence of  $\epsilon$  on the wave vector  $\mathbf{k}$  of the light wave, the new theory predicts the propagation in the crystal of two normal waves having the same frequency and polarization, but different velocities, i.e., different refractive indices.

One of the most important experimental proofs of the validity of the spatial-dispersion theory was the impossibility of describing the optical properties of the CdS crystal at 4.2 K, in light transmitted through the target and reflected from it, by means of a single diffraction index  $n$  and a single absorption coefficient  $\kappa$ , i.e., by a dielectric constant of the form  $\epsilon(\omega) = [n(\omega) + i\kappa(\omega)]^2$ . Thus, it was shown<sup>[2]</sup> that the spectral dependence of the reflection coefficient  $R(\omega)$  calculated from the measured dispersion<sup>[3]</sup> and absorption<sup>[4]</sup> curves differs strongly from that measured in experiment. At the same time, these results can be very well reconciled by using the formulas of the spatial dispersion theory.<sup>[5]</sup> It became recently<sup>[6,7]</sup> possible to measure the phase  $\varphi(\omega)$  of the reflected light in the region of the exciton band  $A$  of the CdS crystal. These results also confirmed the impossibility of describing the behavior of  $\varphi(\omega)$  at 4.2 K by the formulas of classical optics and the need for resorting to the theory of spatial dispersion to explain the experimental data.

Another no less important confirmation of the essen-

tial role played by spatial dispersion in CdSe and CdS crystals at 4.2 K was the observation of interference of normal waves on the short-wave side of the exciton absorption band<sup>[8]</sup> and the reconstruction, from the obtained interference pattern, of their dispersion relations  $E_1(\mathbf{k})$  and  $E_2(\mathbf{k})$ . It has thus been convincingly shown that the spatial dispersion exerts a significant influence on the optical properties of crystals in the region of exciton absorption bands at temperatures 4.2 K and below. It is known at the same time that at high temperatures the formulas of classical optics are well satisfied, i.e., the spatial-dispersion effects become insignificant.

The temperature dependence of the spatial-dispersion effects in CdS crystals was investigated experimentally by Voigt<sup>[9]</sup> and by Brodin *et al.*<sup>[10]</sup> With increasing temperature, a sharp increase of the area under absorption curve in the region of the exciton band  $A$ <sup>[9]</sup> and a characteristic change of the birefringence picture<sup>[10]</sup> were observed. To explain the results of<sup>[10]</sup>, theoretical calculations performed by Davydov and Myasnikov<sup>[11]</sup> for anthracene crystals were used. But since exciton parameters of CdS and anthracene differ greatly, only qualitative agreement between theory and experiment, and a qualitative description of the general tendency of the variation of the optical characteristic of the substance with increasing temperature, could be expected.

We report here calculations that make it possible to follow the gradual change in various characteristics of both normal waves with increasing damping constant  $\gamma$  of the excitons in CdS crystals. The obtained data are used for a quantitative estimate of  $\gamma$  in various crystals investigated in different experimental conditions. Two

waves with refractive indices having different spectral dependences were observed, for the first time ever, by a direct interference method. It is shown that this takes place if  $\gamma$  of the excitons is close to the "critical" value.

### CALCULATION RESULTS

According to Pekar's theory<sup>[1]</sup> the complex refractive indices of the two normal waves are determined from the relation

$$n_{\pm}^2 = \frac{1}{2} (\mu + \epsilon_0) \pm \left[ \frac{1}{4} (\mu - \epsilon_0)^2 + b \right]^{1/2}, \quad \mu = \mu' + i\mu'' \quad (1)$$

$$\mu' = \frac{2Mc^2}{\hbar\omega_0^2} (\omega - \omega_0), \quad \mu'' = \frac{2Mc^2}{\hbar\omega_0^2} \gamma, \quad b = \frac{4\pi c^2 e^2}{\hbar\omega_0^3} \frac{M}{m} Nf,$$

where  $\epsilon_0$  is the background value of the dielectric constant,  $M$  is the exciton effective mass,  $c$  is the speed of light in vacuum,  $e$  and  $m$  are the charge and mass of the free electron,  $\hbar\omega_0$  is the energy of the bottom of the exciton band,  $f$  is the oscillator strength of the unit crystal cell,  $N$  is the number of cells per unit volume, and  $\gamma$  is the damping constant of the excitons.

Formulas (1) were used to calculate the real ( $n'$ ) and imaginary ( $n''$ ) parts of the refractive indices of both waves ( $n_+$  and  $n_-$ ) for different  $\gamma$ . The values of the remaining parameters that enter in the formulas were taken to be the same as in<sup>[5]</sup>, namely,  $\epsilon_0 = 7.74$ ,  $M = 0.9m$ ;  $b = 1578$  (corresponding to  $f = 0.0021$  or to a longitudinal-transverse splitting  $\Delta\nu_{LT} = 11.8 \text{ cm}^{-1}$ );  $\gamma_0 = 20586.6 \text{ cm}^{-1}$ , and  $\nu = 1/\lambda = \omega/2\pi c$  is the wave number. The calculation results are shown in Fig. 1a.

The ratio of the amplitudes of the normal waves pro-

duced in the crystal and the phase shift between them are determined, according to<sup>[1]</sup>, by the ratio

$$-\frac{E_-}{E_+} = q = |q| e^{i\varphi} = \frac{\epsilon_0 - n_+^2}{\epsilon_0 - n_-^2} \quad (2)$$

The plots of  $\log |q|$  and  $\varphi$  calculated from (2) are shown in Fig. 1b.

The wave reflected at normal incidence can be formally described, provided that the boundary conditions of<sup>[1]</sup> are satisfied, by the equations of the single-wave theory if the so-called "effective" refractive index  $n^* = n^{*eff} + i\kappa^{*eff}$  is introduced. The reflection coefficient is then

$$R = \left| \frac{1 - n^*}{1 + n^*} \right|^2, \quad (3)$$

$$n^* = \frac{n_+}{1 - q} + \frac{n_-}{1 - 1/q} = \frac{\epsilon_0 + n_+ n_-}{n_+ + n_-}.$$

The calculated real ( $n^{*eff}$ ) and imaginary ( $\kappa^{*eff}$ ) parts of  $n^*$  and of  $R$  are shown in Fig. 1c.

Let us discuss the obtained relations in greater detail. It follows from Fig. 1a that at  $\gamma = 0$  the wave  $E_+$  in the entire spectral region and the wave  $E_-$  on the short-wave side of  $\nu_L$  (the frequency of the longitudinal exciton) are undamped, since they have a purely real refractive index. On the long-wave side of  $\nu_L$  the wave  $E_-$  has a pure imaginary refractive index, and is consequently totally reflected from the crystal, after penetrating to only a small depth determined by the corresponding frequency-dependent damping coefficient. There is therefore no true absorption of energy in the crystal. It is seen next from Fig. 1b that the amplitudes of the waves,  $E_+$  and  $E_-$  are equal only near the frequency  $\nu_0$ , and their ratio changes strongly in a

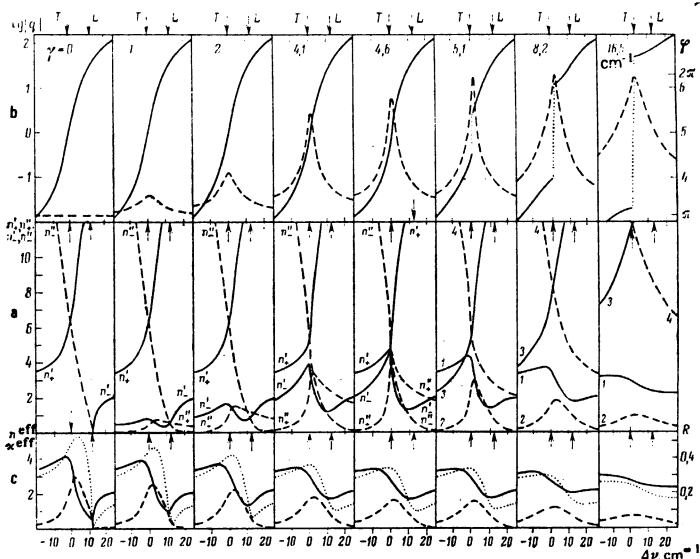


FIG. 1. Frequency dependences calculated theoretically for different values of the exciton damping constant  $\gamma$ : a—for the complex refractive indices of the two normal waves  $E_+$  and  $E_-$  according to formula (1) (the real parts ( $n'_+$  and  $n'_-$ ) are represented by solid lines, and the imaginary parts ( $n''_+$  and  $n''_-$ ) are dashed); b—for the ratios of the amplitudes of the normal waves (in logarithmic scale) and of the phase shift between them according to formula (2) ( $\log |q|$  and  $\varphi$  are represented by the solid and dashed lines, respectively); c—for the real and imaginary parts of the "effective" refractive index and of the reflection coefficient according to formula (3), represented respectively by solid ( $n^{*eff}$ ), dashed ( $\kappa^{*eff}$ ), and dotted ( $R$ ) lines. An arrow  $T$  marks the energy position of the bottom of the band of the transverse excitons, corresponding to a value  $\Delta\nu = 0$  ( $\nu_T = \nu_0$ ) on the abscissa axis. An arrow  $L$  marks the energy position of the longitudinal excitons at  $k = 0$  and  $T = 0$ .

small spectral interval on both sides of  $\nu_0$ : by approximately three orders of magnitude in the interval  $\Delta\nu = 2\Delta\nu_{LT}$ . The wave  $E_+$  dominates on the long-wave side of  $\nu_0$ , and  $E_-$  on the short-wave side. The phase difference between the waves at the crystal boundary, at the instant of excitation by the electromagnetic wave, is equal to  $\pi$  in the entire spectral region. In other words, the waves are in counterphase at the instant of their production.

Under these conditions, with increasing frequency, up to  $\nu_L$ , one should register a virtual absorption in the vicinity of  $\nu_0$ , due to the decrease of amplitude of the wave  $E_+$  and hence the decrease of the energy carried by it, and due to the increase of the amplitude of  $E_-$  and hence of the reflected energy, in the light passing through the crystal. If we determine the refractive index by the usual method from the change of the phase of the light passing through the crystal, then we should obtain, up to the frequency  $\nu_L$ , the dispersion branch of the wave  $E_+$ , followed by a jump over to the branch of the wave  $E_-$ ; the latter has the larger amplitude at the frequency  $\nu_L$ . The form of the reflection spectrum of a semi-infinite crystal should then be such as if one wave were to propagate in the crystal and to have  $n^{eff}$  and  $\chi^{eff}$  with frequency dependences shown in Fig. 1c. In other words, the spectral characteristics of the reflected wave are in no way similar to those of the waves  $E_+$  and  $E_-$  inside the crystal.

We examine now how the characteristics of the two waves change at  $\gamma \neq 0$ , i.e., when true energy absorption appears in the crystal. With increasing frequency dependence of  $n'_+$  acquires with increasing  $\gamma$  an ever increasing sag that lowers the refractive index near the frequency  $\nu_0$ . The frequency dependence of  $n'_-$  acquires a tail-like extension on the short-wave side of  $\nu_L$ . What is new compared with  $\gamma = 0$  is that  $n'_+$  has a strongly asymmetrical bell shape whose maximum increases sharply with increasing  $\gamma$ . Finally, the plot of  $n'_-$  has now a very characteristic continuation into the long-wave side of  $\nu_L$ , namely, a maximum appears at  $\nu_0$  and increases sharply with increasing  $\gamma$ . At a definite value of  $\gamma$ , called in [11] "critical" ( $\gamma_{cr}$ ), the maximum of the  $n'_-$  curve rises to the  $n'_+$  branch, and the refractive indices of both waves become equal at the frequency  $\nu_0$ . With further increase of  $\gamma$  the  $n'_-$  and  $n'_+$  curves intersect, and on going through  $\nu_0$  the two branches of the wave  $E_+$  go over continuously into branches of the wave  $E_-$ :  $n'_+ \rightarrow n'_-$ ;  $n''_+ \rightarrow n''_-$ ;  $n'_- \rightarrow n'_+$ ;  $n''_- \rightarrow n''_+$ . These curves are marked 1, 2, 3, and 4 respectively on the figure. At  $\gamma < \gamma_{cr}$  the amplitudes of both waves are equal at the frequency  $\nu_0$  ( $\log |q| = 0$ ), and above  $\gamma_{cr}$  they differ substantially over the entire spectral band (the  $\log |q|$  curve has a discontinuity at the frequency  $\nu_0$ ), and their difference is larger the larger  $\gamma$ . In addition, it is seen from Figs. 1a and 1b that at  $\gamma > \gamma_{cr}$  the wave having at the instant of production the larger amplitude is less absorbed. It is also seen from Fig. 1b that as  $\gamma$  increases a characteristic peak appears on the spectral dependence of the phase difference between the waves, at the frequency  $\nu_0$ , and its maximum value reaches  $2\pi$ . This shows that in the presence of appreciable absorp-

tion both waves are excited in phase.

Let us see now how the described variations of the curves with increasing  $\gamma$  should affect the absorption and reflection spectra and the spectra of the dispersion of the refractive index of the crystal.

Only qualitative conclusions can be drawn concerning the absorption spectrum, since more exact information can be obtained only after calculating the transparency of a crystal plate with the formulas of [1] and with account taken of the still unknown frequency dependence of  $\gamma(\nu)$ . It follows from Fig. 1b that the spectral dependence of the ratio of the amplitudes of the waves  $E_+$  and  $E_-$  changes insignificantly from  $\gamma = 0$  up to  $\gamma_{cr}$ . At the same time the wave  $E_+$  experiences ever increasing absorption ( $n''_+$  increases). Although the wave  $E_-$  does become complex and thus becomes capable of propagating inside the crystal, it attenuates not much more weakly at  $\gamma < \gamma_{cr}$  than at  $\gamma = 0$ . The absorption of the light passing through the crystal is therefore expected to increase strongly when  $\gamma$  changes from 0 to  $\gamma_{cr}$ . Above  $\gamma_{cr}$ , as already noted, the wave that is less absorbed has also the larger amplitude. The spectral dependences of its refractive index and absorption coefficients are shown by curves 1 and 2, respectively, and have the usual classical form. The area under the absorption curve under these conditions, taking into account the decreased contribution of the wave that is more absorbed, should no longer change with further increase of  $\gamma$ , since the broadening of the curve is offset by the lowering of its maximum.

We trace now the variation of the dispersion of the refractive index of the crystal, as determined by measuring the phase of the light passing through the crystal. At small  $\gamma(1 - 2 \text{ cm}^{-1})$ , before the absorption of the wave  $E_+$  has grown strong enough, the picture should be almost the same as at  $\gamma = 0$ , i.e., a dispersion branch  $n'_+$  and then an abrupt jump to the branch  $n'_-$ . With further increase of  $\gamma$ , as  $\gamma_{cr}$  is approached, the absorption coefficients of both waves  $E_+$  and  $E_-$  become comparable in the spectral region of the longitudinal-transverse splitting, and therefore the intensities of both waves increase at the exit from the crystal. Two branches of the refractive index should therefore be registered: one increasing and pertaining to the wave  $E_+$ , and the other decreasing and pertaining to the wave  $E_-$ . Finally, when  $\gamma$  exceeds  $\gamma_{cr}$  and only one wave becomes dominant in the transmitted light, the dispersion wave should have the usual classical form with an "anomalous" section in the region of the absorption band. Thus, with increasing  $\gamma$  the dispersion curves should undergo within the limits of the absorption band the following transformation: 1) at small  $\gamma$ —one rapidly growing branch  $n'_+$  followed by a jump to branch  $n'_-$ ; 2) at  $\gamma \approx \gamma_{cr}$ —coexistence of two branches, one rising ( $n'_+$ ) and the other falling ( $n'_-$ ); 3) at  $\gamma > \gamma_{cr}$ —one falling branch (1) corresponding to the section of "anomalous" dispersion.

We proceed now to the reflection spectra. When  $\gamma$  increases all have the usual classical form, as if one wave with the effective refractive index shown in Fig. 1c were to propagate in the crystal. From the form of the  $R(\nu)$  curves we cannot determine how many waves

having the same frequency and polarization propagate inside the crystal. In other words, there are two situations that are indistinguishable in principle: there propagate in the medium either two waves with the characteristics shown in Fig. 1a, or else one wave with the constants of Fig. 1c.

The reflection spectra shown in Fig. 1c can be obtained, naturally, only if the sample surface is perfect and the boundary conditions of [1] are satisfied. It is well known that in the presence of a "dead" layer [12] or of a spoiled surface the reflection spectrum takes another form, but we shall not dwell on this question.

Comparison of Figs. 1a and 1c show that curves 1 and 2, with increasing  $\gamma$  in the region above  $\gamma_{cr}$  come closer and closer, in general form and in swing amplitude, to the  $n^{eff}$  and  $\kappa^{eff}$  curves, until they ultimately merge with the latter. This means that the effects of spatial dispersion vanish completely, and all the optical properties of the crystal can be described by the one-wave theory. In CdS this takes place at  $\gamma \approx 16 \text{ cm}^{-1}$ .

### COMPARISON WITH EXPERIMENT

We shall attempt to use the aggregate of the presented curves to estimate the values of  $\gamma$  in particular crystals.

The absorption spectra of CdS crystals at various temperatures (4–77 K) were measured in [9,13]. The samples investigated in [13] were clamped and the area under the absorption curve was found to be independent of  $T$ . In [9], where the samples were "free," the experimental dependence was precisely the one which followed from an analysis of the theoretical curve, namely, an abrupt increase of the area under the absorption curve with increasing  $T$  at low temperatures, and stabilization of the area at high temperatures. This shows that the value of  $\gamma$  of clamped samples is not less than  $\gamma_{cr}$  even at 4.2 K, whereas  $\gamma_{4.2} \ll \gamma_{cr}$  in the "free" samples.

The dispersion of the refractive index of CdS at 4.2 K was measured in "free" thin crystals [3] by two independent methods. In the first, a Jamin interferometer was crossed with a spectrograph, and the obtained interference pattern traced, to a definite scale, the spectral dependence of the refractive index (Fig. 2a). In the second method the birefringence of the crystal was used together with the interference of beams with polarizations  $\mathbf{E} \parallel \mathbf{C}$  and  $\mathbf{E} \perp \mathbf{C}$ . A distinct pattern of alternating maxima and minima was observed (Figs. 2d and 2e), and from their spectral positions it was possible to calculate the courses of the branches  $n'_+$  and  $n'_-$ , each for its own spectral interval. Both methods yielded the dispersion curve expected theoretically at small  $\gamma \ll \gamma_{cr}$  (Fig. 3a). Comparison of this curve with the theoretical one of [5] yielded  $\gamma_{4.2} \approx 2 \text{ cm}^{-1}$ .

The temperature dependence of  $n(\lambda)$  was investigated [10] on the same crystals only by the second method. With increasing temperature, a successive vanishing of the interference extrema corresponding to the  $E_+$  branch was observed, starting with the shortest wavelength and

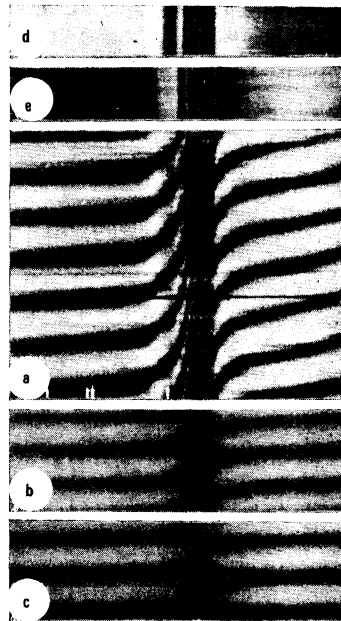


FIG. 2. Birefringence in parallel (d) and crossed (e) polarizers and interference pattern (a), obtained with a "free" CdS crystal  $0.34 \mu\text{m}$  thick at 4.2 K. Interference patterns of clamped sample  $0.095 \mu\text{m}$  thick at 20 K (b) and 77 K (c). The three presented interference patterns illustrate, as it were, the three different cases:  $\gamma \ll \gamma_{cr}$ ,  $\gamma \approx \gamma_{cr}$ , and  $\gamma \gg \gamma_{cr}$ .

gradually propagating to the long-wave side. At 77 K the birefringence picture corresponded already to the classical dispersion curve, i.e.,  $\gamma > \gamma_{cr}$ .

From the examination of the theoretical curves above we expect precisely such a behavior of the birefringence picture. Distinct interference fringes are obtained when only one wave with definite phase passes through the crystal in the spectrum component  $\mathbf{E} \perp \mathbf{C}$ , i.e., at small and at large  $\gamma$ . In the intermediate region, as the amplitudes of the waves  $E_+$  and  $E_-$  at the exit from the crystal begin to equalize with increasing  $\gamma$ , the phase of the resultant wave passing through the crystal turns out to be a complicated function of the refractive indices of both waves and of the crystal thickness. In fact, in one case, when two harmonic oscillations of equal frequency but with different phases [ $a \cos(\omega t + \varphi_1)$  and  $(b \cos \omega t + \varphi_2)$ ] are added, harmonic oscillations of the same fre-

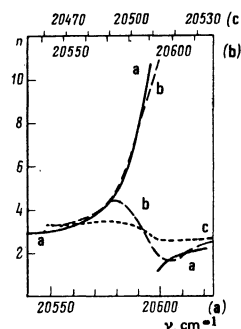


FIG. 3. Dispersion curves of a CdS crystals, calculated from the interference patterns (a), (b), and (c) of Fig. 2. To facilitate the comparison, they are shifted along the frequency scale until the corresponding spectral positions of the band A coincide.

quency,  $x \cos(\omega t + \psi)$  is obtained, and its amplitude and phase are given by

$$\begin{aligned} x^2 &= a^2 + b^2 + 2ab \cos(\varphi_1 - \varphi_2), \\ \operatorname{tg} \psi &= \frac{a \sin \varphi_1 + b \sin \varphi_2}{a \cos \varphi_1 + b \cos \varphi_2}. \end{aligned} \quad (4)$$

It follows from these formulas that  $\psi$  has a value intermediate between  $\varphi_1$  and  $\varphi_2$ , and it is closer to  $\varphi_1$  (or  $\varphi_2$ ) the larger the ratio  $a/b$  (or  $b/a$ ). In the limit,  $\psi \rightarrow \varphi_1$  as  $b \rightarrow 0$  and  $\psi = (\varphi_1 + \varphi_2)/2$  at  $a = b$ . Consequently, with increasing amplitude of the wave  $E_-$  at the exit from the crystal, the phase of the resultant wave decreases and differs all the more from the phase difference for only the wave  $E_+$ . Given the crystal thickness, this corresponds, as it were, to a decrease of its refractive index. Therefore when the temperature is raised in birefringence experiments the phase shift of the resultant wave is no longer sufficient for the formation of the corresponding interference extremum. The extrema begin to vanish gradually, starting with the frequency  $\nu_L$  and going to the long-wave side, since this is where the increase of the amplitude of  $E_-$  begins to increase relative to  $E_+$  with increasing  $\gamma$ .

The degree to which the contribution of the  $E_-$  wave affects the resultant phase depends on the sample thickness, for when the input amplitudes and the damping coefficients of the  $E_+$  and  $E_-$  waves are given the thickness is the dominant factor in the ratio of their amplitudes as they emerge from the crystal. In this context it was noted<sup>[10]</sup> that the concept of the refractive index as a bulk characteristic of a substance ceases to be definite in the region of  $\gamma_{cr}$ .

On the basis of the foregoing reasoning, we can expect that if the phase change of the light passing through the crystal is measured with an interferometer crossed with a spectrograph, under conditions when the corresponding value of  $\gamma$  is close to  $\gamma_{cr}$ , then the change should correspond, within the limits of the absorption band, to a refractive index intermediate between  $n'_+$  and  $n'_-$ . Furthermore, this averaged value is closer to the  $n'_+$  branch near  $\nu_T$  and to  $n'_-$  near  $\nu_L$ .

The experimentally obtained interference pattern for a crystal under conditions close to  $\gamma_{cr}$  has shown, however, a different picture, that of Fig. 2b. Within the limits of the absorption bands, the interference fringes are split despite their low sharpness.<sup>1)</sup> The growing branch is steeper, and its maximum upward displacement from the splitting point amounts to approximately 1.5 fringes; the decreasing branch is more gently sloping, and its maximum downward displacement is about one-half a fringe.

If we use this interference pattern to calculate the dispersion of the refractive index, including the splitting region, then the obtained picture (Fig. 3b) is very close to the theoretically predicted course of the branches  $n'_+$  and  $n'_-$  near  $\gamma_{cr}$  (Fig. 1a). If we recognize that curves  $a$  and  $b$  of Fig. 3 were obtained for crystals of different thickness, at different temperatures, and differently deformed, then their good agreement on the rising section is striking. This behavior, however,

with the exception of the small sag, is predicted by the theory for  $\gamma$  varying from 0 to  $\gamma_{cr}$  (Fig. 1a). The values of  $n$  obtained for the descending branch of the curve of Fig. 3 are also quite reasonable and in good agreement with the theory. This result can hardly be regarded as accidental. We are forced to conclude that the registered behavior of the interference fringes corresponds to the true dispersion of the branches  $n'_+$  and  $n'_-$  inside the crystal. We are left, however, with the question why the wave passing through the crystal carries separate phase information on the waves  $E_+$  and  $E_-$  rather than information on the resultant combined wave.<sup>2)</sup>

To complete the picture, Fig. 2c shows an interference pattern of a crystal under conditions  $\gamma > \gamma_{cr}$ , while Fig. 3c shows the dispersion curve calculated from it. It can be described by the usual one-wave theory.

From the comparison of the curves of Fig. 3 with Fig. 1a we can estimate approximately the values of  $\gamma$  for all three cases:  $\gamma_{4.2} \approx 1 \text{ cm}^{-1}$ ,  $\gamma_{20} \approx 4.6 \text{ cm}^{-1}$ , and  $\gamma_{77} \approx 16.5 \text{ cm}^{-1}$ . Investigations<sup>[7]</sup> of the phase of light reflected by "thick" "free-standing" CdS crystals yielded  $\gamma_{4.2} \approx 1.4 \text{ cm}^{-1}$  and  $\gamma_{77} \approx 4.3 \text{ cm}^{-1}$ . This confirms an earlier conclusion<sup>[10]</sup> that the values of  $\gamma$  of different samples can differ significantly at the same temperatures, depending on the degree of perfection of the samples. Particularly significant are the method of securing the crystal and its deformation:  $\gamma$  of clamped samples are several times (2–4) larger than  $\gamma$  of "free" ones. This takes them immediately into the region above  $\gamma_{cr}$ , i.e., to conditions when spatial-dispersion effects cease to matter.

<sup>1)</sup>A similar splitting of interference fringes ("forks") were observed for a number of crystals back in 1959. <sup>[14]</sup>

<sup>2)</sup>Incidentally, if the waves  $E_+$  and  $E_-$  were to interfere independently with the wave  $E_0$  in birefringence experiments, then the interference fringes would likewise fade out with increasing temperature, owing to superposition of another pattern with different spectral positions of the extrema.

<sup>3)</sup>S. I. Pekar, Zh. Eksp. Teor. Fiz. 33, 1022 (1957); 34, 1176 (1958); 36, 451 (1959) [Sov. Phys. JETP 6, 785 (1958); 7, 813 (1958); 9, 314 (1959)].

<sup>4)</sup>M. I. Strashnikova, Fiz. Tverd. Tela (Leningrad) 17, 729 (1975) [Sov. Phys. Solid State 17, 467 (1975)].

<sup>5)</sup>M. S. Brodin, N. A. Davydova, and M. I. Strashnikova, Pis'ma Zh. Eksp. Teor. Fiz. 19, 567 (1977) [JETP Lett. 19, 324 (1977)].

<sup>6)</sup>M. I. Strashnikova and A. T. Rudchik, Fiz. Tverd. Tela (Leningrad) 14, 984 (1972) [Sov. Phys. Solid State 14, 845 (1972)].

<sup>7)</sup>S. I. Pekar and M. I. Strashnikova, Zh. Eksp. Teor. Fiz. 68, 2047 (1975) [Sov. Phys. JETP 41, 1024 (1975)].

<sup>8)</sup>L. E. Solov'ev and A. V. Babinskiĭ, Pis'ma Zh. Eksp. Teor. Fiz. 23, 291 (1976) [JETP Lett. 23, 263 (1976)].

<sup>9)</sup>A. V. Komarov, S. M. Ryabchenko, and M. I. Strashnikova, Zh. Eksp. Teor. Fiz. 74, 251 (1978) [Sov. Phys. JETP 47, No. 1 (1978)].

<sup>10)</sup>V. A. Kiselev, B. S. Razbirin, and I. N. Ural'tsev, Pis'ma Zh. Eksp. Teor. Fiz. 18, 504 (1973) [JETP Lett. 18, 296 (1973)]; V. A. Kiselev, B. S. Razbirin, and I. N. Ural'tsev, Phys. Status Solidi B 72, 161 (1975).

<sup>11)</sup>J. Voigt, Phys. Status Solidi B 64, 549 (1974).

<sup>12)</sup>M. S. Brodin, N. A. Davydova, and M. I. Strashnikova,

## Electron-hole drop radiation in the far infrared part of the spectrum

T. M. Bragina, Yu. S. Lelikov, Ya. E. Pokrovskii, K. I. Svistunova, and Yu. G. Shreter

A. F. Ioffe Physicotechnical Institute, Academy of Sciences of the USSR, Leningrad

(Submitted 23 December 1977)

Zh. Eksp. Teor. Fiz. 74, 2215-2219 (June 1978)

It was established experimentally that the effects attributed earlier to electron-hole drops in the far infrared may, in fact, be due to the room-temperature background radiation modulated by resonant absorption in the drops.

PACS numbers: 71.35.+z, 78.30.-j

Vavilov, Zayats, and Murzin<sup>[1,2]</sup> reported the discovery of resonant emission of submillimeter radiation at the plasma frequency of electron-hole drops in germanium. To explain the physical nature of this effect, we proposed<sup>[3]</sup> a mechanism of the excitation of plasma oscillations by fast Auger electrons resulting from carrier recombination in electron-hole drops. Further detailed investigations were desirable to determine the role of this mechanism. However, our attempts to observe drop radiation were unsuccessful although it was reported by Zayats<sup>[2]</sup> that the integrated intensity of the radiation amounted to  $10^{-7}$  W/cm<sup>2</sup>. In the present paper we shall give experimental evidence suggesting that the phenomenon discovered by Vavilov *et al.*<sup>[1,2]</sup> could be due not to the emission but to resonant absorption of the room-temperature background radiation by the drops.

In the first series of experiments we recorded submillimeter radiation using a photoresistor made of silicon doped with boron in a concentration of  $\approx 5 \times 10^{14}$  cm<sup>-3</sup>. At helium temperatures and under the action of impurity-absorbed illumination of wavelength shorter than  $30\mu$  the optical charging of neutral boron atoms in silicon produced the  $A^*$  centers with an ionization energy of about 3 meV (the spectral range of the detector extended to  $500\mu$ , with a sensitivity maximum at  $300\mu$ <sup>[4]</sup>). The threshold sensitivity of our device in the 100-400 $\mu$  range was at least  $5 \times 10^{-13}$  W/Hz<sup>1/2</sup> at 1.6 °K. Under the experimental conditions (Fig. 1) the source of the impurity-absorbed illumination necessary for the operation of the detector 1 was the room-temperature background radiation 5 which passed along a stainless-steel tube 2. Samples of pure (with an impurity concentration  $N \approx 10^{11}$  cm<sup>-3</sup>) and doped ( $N \approx 5 \times 10^{14}$  cm<sup>-3</sup>) germanium 4 were excited with modulated radiation from an argon laser 6 whose power was up to 150 mW and which was focused on a sample in the form of a spot  $\approx 5$  mm in diameter. The formation of drops in the samples was de-

duced from the recombination radiation (luminescence) spectrum. The photodetector was protected from the exciting and recombination radiations by a filter 3 made of indium antimonide, 2 mm thick, and black polyethylene. The experiments were carried out at temperatures below 2.1 °K. Two relative positions of the germanium sample and photodetector were tried. In the first case (Fig. 1a) the background radiation passed first through the photodetector and then through the germanium plate. Under these conditions we observed no photoresponse from the detector even at the highest rate of excitation of germanium. Since under our conditions the sensitivity of the photodetector to submillimeter radiation was at least as high as in the work of Vavilov *et al.*<sup>[1,2]</sup> we concluded that the long-wavelength radiation emitted from drops in germanium could hardly have been discovered by Vavilov *et al.*<sup>[1,2]</sup> In the second case (Fig. 1b, when the background radiation first passed through germanium and then through the photodetector, we recorded a photoresponse which was approximately three orders of magnitude higher than

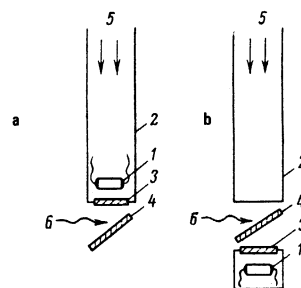


FIG. 1. Schematic diagrams of the experimental set up employing a boron-doped silicon detector: 1) photodetector; 2) stainless-steel tube; 3) filter made of indium antimonide and black polyethylene; 4) germanium sample; 5) background radiation; 6) exciting radiation.